Self-Assembled Fibers

DOI: 10.1002/ange.201308795

Multi-Colored Fibers by Self-Assembly of DNA, Histone Proteins, and Cationic Conjugated Polymers**

Fengyan Wang, Zhang Liu, Bing Wang, Liheng Feng, Libing Liu, Fengting Lv, Yilin Wang,* and Shu Wang**

Abstract: *The development of biomolecular fiber materials with imaging ability has become more and more useful for biological applications. In this work, cationic conjugated polymers (CCPs) were used to construct inherent fluorescent microfibers with natural biological macromolecules (DNA and histone proteins) through the interfacial polyelectrolyte complexation (IPC) procedure. Isothermal titration microcalorimetry results show that the driving forces for fiber formation are electrostatic and hydrophobic interactions, as well as the release of counterions and bound water molecules. Color-encoded IPC fibers were also obtained based on the co-assembly of DNA, histone proteins, and blue-, green-, or red-(RGB-) emissive CCPs by tuning the fluorescence resonance energy-transfer among the CCPs at a single excitation wavelength. The fibers could encapsulate GFP-coded Escherichia coli BL21, and the expression of GFP proteins was successfully regulated by the external environment of the fibers. These multi-colored fibers show a great potential in biomedical applications, such as biosensor, delivery, and release of biological molecules and tissue engineering.*

Polyion complexes are formed by self-assembly of two oppositely charged polyelectrolytes in aqueous solution. They have been widely used in constructing membranes, antistatic coatings, surfactants, and microcapsules.[1–4] The polyion complexes could form fibers at an interface through an interfacial polyelectrolyte complexation (IPC) process.[5,6] Chromatin is one perfect example of natural IPC fibers formed through self-assembly of oppositely charged DNA and histone proteins. Although IPC fibers composed of many different polyelectrolytes have been extensively studied,[7] fibers constructed by natural biological macromolecules have been rarely reported.[8] IPC fibers possess good biocompatibility and are attractive materials for biomedical applications, such as biosensors,[9] delivery of biological molecules,[8,10] encapsulation of cells, and tissue engineering.[7a,11] Recently, biomaterials with imaging ability have become more and more useful because one can monitor biological processes and visualize the medical imaging for diagnosis and therapy. Until now, the reported way to make fluorescent IPC fibers has been to incorporate or stain them with organic dyes or quantum dots (QDs).[7a,8] However, fluorescent dyes usually suffer from photobleaching,[12] and QDs are cytotoxic because of the leaking of heavy metals from their nanocrystal core.[13] These facts provide the motivation for designing new inherent fluorescent IPC fibers.

Cationic conjugated polymers (CCPs) can form complexes with negatively charged DNA through electrostatic interactions, which have been widely used for highly sensitive DNA detection.[14,15] They exhibit high fluorescence brightness, excellent photostability, and lower toxicity,[16] thus fabrication of fluorescent IPC fibers with CCPs, DNA, and histone proteins are expected. Herein we synthesized four CCPs (PFP, PPE, PT, and PBF) that exhibit blue, green, orange, and red fluorescent emissions, respectively. These CCPs could respectively form inherent fluorescent microfibers with natural salmon sperm DNA and histone proteins through the IPC procedure. Color-encoded IPC fibers could also be prepared through co-assembly of DNA, histone proteins, and RGB-emissive CCPs. We further encapsulated GFP-coded *Escherichia coli* BL21 into the DNA/histone/CCPs IPC fibers, and the expression of GFP proteins was successfully regulated in the external environment of the fibers.

Four CCPs (PFP, PPE, PT, and PBF) with different fluorescent colors (blue, green, orange, and red) were used. Their chemical structures are shown in Scheme 1 A. PFP[17] and PBF[18] were prepared according to the previous procedures. The synthesis of PPE is illustrated in Scheme 1 B. Boc-PPE was prepared by copolymerization of **1** and **2** through a Sonogashira coupling reaction. Then, deprotection of the *tert*-butoxycarbonyl group affords PPE. The synthesis of PT is outlined in Scheme 1 C. Treatment of 2-(thiophen-3-yl)ethyl 4-methylbenzenesulfonate (**3**) with NaH and triethylene glycol in anhydrous THF affords 3-(2-(2-(2-hydroxyethoxy)ethoxy)ethoxy)ethylthiophene (**4**) in 23% yield. Reaction of **4** and 4-methylbenzene-1-sulfonyl chloride in the presence of pyridine in CH_2Cl_2 provides 2-(2-(2-(2-(thiophen-3-yl)ethoxy)ethoxy)ethoxy)ethyl 4-methylbenzenesulfonate (**5**) in 92% yield. Treatment of **5** with $LiBr{\cdot}H_2O$ in acetone gives 3-(2-(2-

[*] F. Wang, B. Wang, Dr. L. Feng, Prof. L. Liu, Prof. F. Lv, Prof. S. Wang
Beijing National Laboratory for Molecular Sciences
Key Laboratory of Organic Solids
Chinese Academy of Sciences, Beijing 100190 (P. R. China)
E-mail: liulibing@iccas.ac.cn
wangshu@iccas.ac.cn
Z. Liu, Prof. Y. Wang
Beijing National Laboratory for Molecular Sciences
Key Laboratory of Colloid, Interface
and Chemical Thermodynamics, Institute of Chemistry
Chinese Academy of Sciences, Beijing 100190 (P. R. China)
E-mail: yilinwang@iccas.ac.cn

[**] The authors are grateful to the National Natural Science Foundation of China (grant numbers 21033010 and TRR61) and the Major Research Plan of China (grant numbers 2011CB932302 and 2012CB932600).

Supporting information for this article is available on the WWW under http://dx.doi.org/10.1002/anie.201308795.

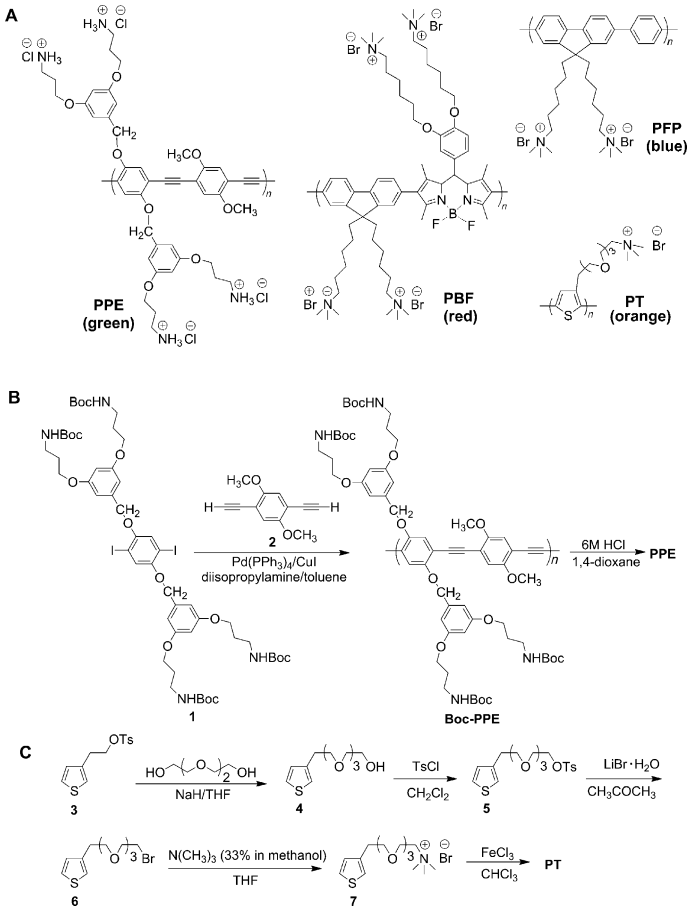

Scheme 1. A) Chemical structures of four CCPs (PFP, PPE, PT, and PBF) that exhibit blue, green, orange, and red fluorescent emissions, respectively. B–C) Synthetic routes of PPE and PT.

(2-(2-bromoethoxy)ethoxy)ethoxy)ethyl)thiophene (**6**) in 88% yield. Then, treatment of **6** with trimethylamine (33% in methanol) in THF offers *N*,*N*,*N*-trimethyl-2-(2-(2-(2-(thiophen-3-yl)ethoxy)ethoxy)ethoxy) ethanaminium bromide (**7**) in 97% yield. Oxidative copolymerization of **7** in nitrogen in the presence of $FeCl_3$ gives PT in 12% yield. Because of the quaternized amine-terminated groups in the side chains, the four CCPs are all soluble in water. Their photophysical properties were measured in aqueous solution and are summarized in Table S1 (see the Supporting Information). PPE exhibits a maximum absorption at 436 nm with a molar extinction coefficient of $3.58 \times 10^4\,M^{-1}\,cm^{-1}$, corresponding to the π–π* transition of the back bone. Its emission displays a maximum peak at 514 nm with a fluorescence quantum yield (QY) of 8.8%. The maximum absorption wavelength of PT is 410 nm with a molar extinction coefficient of $0.32 \times 10^4\,M^{-1}\,cm^{-1}$, and the emission maximum is 565 nm with a QY of 3.5%. From the normalized UV/Vis absorption and fluorescent emission spectra (Figure S1), we could see that the blue-emissive polymer acts as the donor for green-emissive and red-emissive polymers, the green-emissive polymer acts as the acceptor for the blue-emissive one and the donor for the red-emissive one, while the red-emissive polymer acts as the acceptor for the green-emissive and red-emissive polymers. Therefore, if the distance between these CCPs is close enough, intermolecular multi-stepped fluorescence resonance energy transfer (FRET) will occur between them upon excitation of the blue-emissive polymer with a short excitation wavelength.[19]

Composed mainly of negatively charged DNA and positively charged histone proteins, chromatin can be regarded as an example of a natural IPC fiber. To obtain IPC fibers with good biocompatibility like chromatin, DNA and histone proteins were chosen as two primary materials. As shown in Figure 1 A, using a pair of tweezers in a continuous upward movement, we could draw straight IPC fibers from the interface of positively charged histone proteins (H) and negatively charged DNA solutions. Using 5 μL of droplets of polyelectrolyte solution, fibers could be up to a length of 30 cm. IPC fibers constructed with DNA/H/PT and DNA/PT were also fabricated using the same method as that of DNA/H. Light microscope images in Figure 1 B show the morphology of these fibers. The most obvious feature of these fibers is that beadlike structures are distributed periodically along the fiber axis. When freshly drawn these beads took the form of viscous fluid droplets, but then became protuberances upon drying. These beads probably have been formed because of accumulation of water droplets, as discovered in spider silk and artificial fibers which mimic the natural structure of spider silk.[20] Diameters of these fibers are in the range from several to ten micrometers, which probably depends on both components and drawing rate. Field-emission scanning electron microscope (FSEM) images in Figure 1 C demonstrate the surface morphology of these fibers. On the surface of these fibers, parallel ridges and valleys were observed, as noticed by others.[8] However, the roughness extent of these surfaces is different from them. The phenomenon may be attributed to the surface tension of the composing polyelectrolyte solutions. Furthermore, we used the other three CCPs (PFP, PPE and PBF) to make DNA/H/CCPs fibers with blue, green, and red emission colors, respectively. Confocal laser scanning microscopy (CLSM) images show that the fluorescence of CCPs is uniformly distributed in the fibers (Figure 1 D).

To study the formation mechanism of DNA/H/CCP fibers at a microlevel, we used isothermal titration microcalorimetry (ITC) technique[21] to study the interactions among different components of these fibers. We selected PFP and PT as two examples of the four CCPs in the following research. Firstly, we studied the interactions between DNA and CCPs. Figure S2 A shows the changing of the observed enthalpy (ΔH_{obs}) when DNA (1.52 mM) is titrated into the solution of PT (0.34 mM in RU (repeat unit)). When the molar ratio of DNA to PT is less than 0.8, the ΔH_{obs} values is negative and displays a platform, which indicates that the interaction between DNA and PT is an exothermic process, and electrostatic binding between DNA and PT is the dominant force accompanied with the release of counterions and dehydration. When the DNA/PT molar ratio goes beyond 0.8, phase separation occurs. The exothermic ΔH_{obs} increases with further addition of DNA, and it reaches a maximum when the molar ratio reaches to 1.2. At this point, the precipitation process is over,

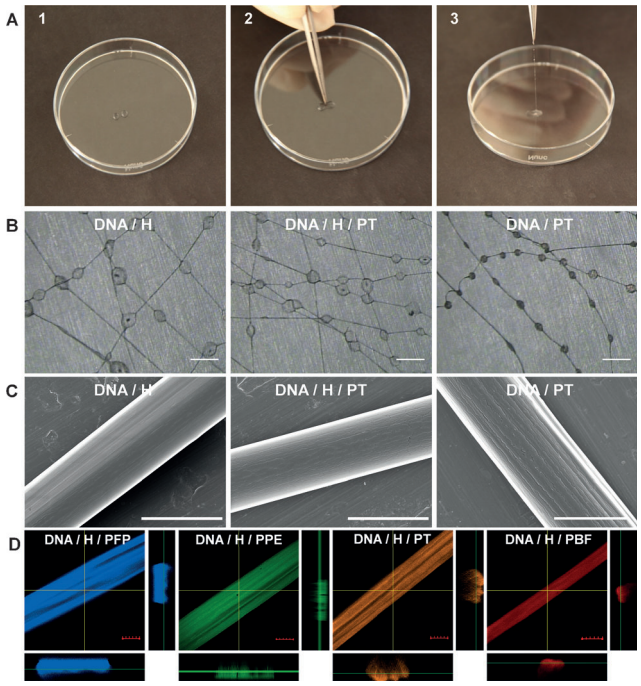

Figure 1. A) Photographs of the IPC fiber drawing process. polyanion: DNA; polycation: H. Light microscope images (B; scale bars 500 μm) and FSEM images (C; scale bars 10 μm) of the IPC fibers: DNA/H, DNA/H/PT ([PT] = 0.2 mg mL^{-1}) and DNA/PT ([PT] = 8 mg mL^{-1}). D) Confocal laser scanning microscopy images of the IPC fibers of DNA/H/CCP (PFP, scale bar 10 μm; PPE, scale bar 30 μm; PT scale bar 10 μm; PBF, scale bar 10 μm; each 0.2 mg mL^{-1}). [DNA] = [H] = 8 mg mL^{-1}. All colors are false colors in these images.

which suggests that PT is fully bound with DNA and the point signifies the saturation of the interaction between them. According to this consideration, we identified the fitting line (Figure S3 A) of the interaction between DNA and PT by assuming that the enthalpy change for the binding became zero at this point. After this molar ratio, further addition of DNA only generates dilution enthalpy. In brief, with the gradual addition of DNA into the system, the ΔH_{obs} curves experience a three-step process: an exothermic platform, a strong exothermic process and a dilution process, which correspond to a gradual combination of DNA with PT, phase separation of DNA/PT complexes, and the dilution of DNA, respectively. Figure S2B shows the ΔH_{obs} change when DNA (1.52 mM) is titrated into the solution of PFP (0.17 mM in RU). It also experienced a three-step process similar to the DNA/PT system. However, different from the DNA/PT system, ΔH_{obs} is positive as DNA was added progressively. This is because the heat released when DNA/PFP is formed by electrostatic binding is overcome by the heat absorbed when the counterions and bound water molecules are released. By fitting the ΔH_{obs} curves using the method described in the Supporting Information, the binding model, binding constant (K), and binding enthalpy (ΔH) are obtained as shown in Table S2. Moreover, the Gibbs free-energy (ΔG) is calculated from $\Delta G = -RT\ln K$ and the entropy change (ΔS) from $T\Delta S = \Delta H - \Delta G$. The binding ratio is 1:1 for the DNA/PT system, and 1:2 for DNA/PFP system, corresponding to the charge ratio of the two systems respectively, so electrostatic interaction is the major interaction. The binding constant is 1.36×10^6 M^{-1} for the DNA/PT system, 3.74×10^{11} M^{-2} for the DNA/PFP system, so it is obvious that the binding ability of DNA with PFP is stronger than that with PT. Moreover, the binding of DNA and PT is an enthalpy–entropy double driven process, because ΔH is negative and $T\Delta S$ is positive in this system. However, because of the positive ΔH and $T\Delta S$, the binding of DNA and PFP is entropy-driven but opposed by the enthalpy. Furthermore, interactions between DNA and H or H and CCP mixtures were studied. As shown in Figures S4 and S5, the DNA/H system also undergoes a three-step progress, an endothermic platform, a strong exothermic process, and a dilution process, similar to the DNA/PT system. But when DNA is added into the mixed solution of H and PT, the system exhibits an exothermic process (Figure S4 A). The phenomenon suggests the interaction of DNA and PT is a strong exothermic process. The variation of the ΔH_{obs} curves means that the interaction between DNA and the mixture of H and PT solution may contain two binding processes. The first process shows a turning point at the molar ratio of 0.015, corresponding to the molar ratio of DNA and PT mixed in H solution. Thus, this binding process is primarily aroused by the interaction between DNA and PT. The second process beyond the molar ratio of 0.015 and before the phase separation indicates the interactions among DNA, H, and PT. Similar with the DNA/PT system, as the molar ratio increases, the DNA/H/PT system also goes through a three-step process and phase separation arises as well. Figure S4 B shows that interactions in DNA/H/PFP system are similar to that in the DNA/H/PT system. However, the interaction between DNA and PFP is an endothermic process, so the endothermic enthalpy of DNA and the mixture of H and PFP is larger than that of DNA and H alone. In summary, the interactions in the DNA/H/CCP system may contain electrostatic and hydrophobic interactions, and the release of counterions and bound water molecules. Using the fitting method mentioned above, we obtained the binding ratio (N), the binding constant (K), the binding enthalpy (ΔH), the Gibbs free-energy (ΔG), and the entropy change (ΔS) of the two systems (Table S3). The fitting results indicate that the interactions in both DNA/H/PT and DNA/H/PFP systems contain two binding processes. From this table we could see that the binding ratio of DNA and H is 0.11 and the binding constant of them is much less than that of DNA with PT or PFP (Table S2), in other words the binding strength of them is far smaller than that of DNA with PT or PFP. Compared with the binding constant of DNA/PT and DNA/H, the K_1 and K_2 values decline for both DNA/H/PT and DNA/H/PFP systems. But in the DNA/H/PFP system, K_1 declines and K_2 is enhanced. The disparity may relate to the hydrophobicity difference of PFP and PT. The aforementioned ITC data analysis indicates the occurrence of binding and phase separation processes.[6]

As the CCPs could be incorporated into the IPC fibers successfully, and intermolecular multi-stepped FRET between them can occur upon the excitation of blue-emissive polymer, we prepared color-encoded IPC fibers based on the co-assembly of DNA, histone proteins, and CCPs. To simplify

names, a new nomenclature is introduced; DNA/H/CCPs fibers with different molar ratios of the CCPs are defined as *m*B*n*G*k*R, where the B, G, and R stand for PFP, PPE, and PBF, respectively, and *m*, *n*, and *k* stand for the molar ratio of them. Red (R), green (G), and blue (B) are three primary colors of light, and mixing them in different proportion could produce a wide variety of emission colors. As shown in Figure 2, we can easily prepare various color-barcoded fibers

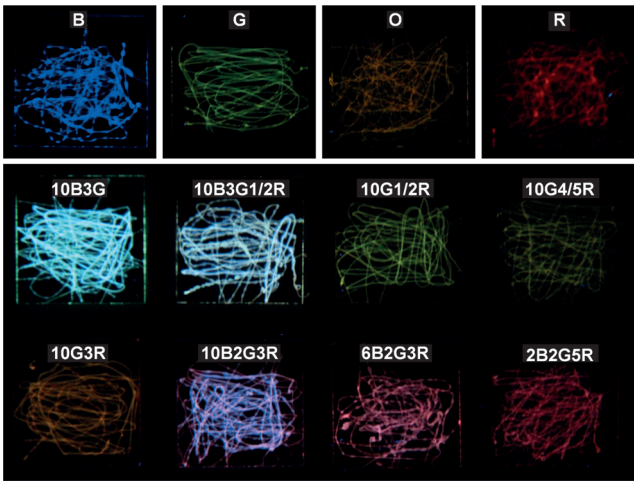

Figure 2. Images of multi-colored fibers fabricated with different concentrations of the four CCPs were taken at 365 nm UV-light irradiation. They were constructed by DNA/H/CCPs. [DNA] = [H] = 8 mg mL^{-1}, [CCPs] = 0.4 mg mL^{-1}. B, G, O, and R stand for PFP, PPE, PT, and PBF, respectively. Parameters of these images: (B) exposure time (1/4 s), aperture (F/5.6), sensitivity (ISO 1600); (R) exposure time (7 s), aperture (F/5.6), sensitivity (ISO 6400); (the others) exposure time (1/4 s), aperture (F/5.6), sensitivity (ISO 6400).

by just incorporating different molar ratios of the three CCPs into the fibers at a single excitation wavelength (365 nm). The emission spectra of the color-barcoded fibers were measured to evaluate the occurrence of multi-stepped FRET. As shown in Figure S6, for the color-barcoded fibers, when the donor is excited, the efficient FRET from donor to acceptor polymers causes a remarkable quenching of the donor and the appearance of acceptor emission. Taking B/G/R fibers as examples, when they are excited at 380 nm (maximum excitation wavelength of PFP), multi-stepped FRET occurs, FRET from PFP to PPE, then FRET from PPE to PBF and direct FRET from PFP to PBF, respectively. These results also show that the fluorescence intensities of PFP, PPE, and PBF components in the fibers are different by varying the ratios of the three CCPs. In other words, the colors can be regulated through fine-tuning the molar ratios of CCPs.

The IPC procedure is carried out at room temperature and in aqueous solutions, thus the resulted fibers possess good biocompatibility. In order to detect the biocompatibility of the newly constructed multi-colored IPC fibers, we encapsulated GFP-coded *Escherichia coli* BL21 cells into DNA/H/PT fibers, and used IPTG (isopropyl-D-1-thiogalactopyranoside) which can induce the GFP gene to express the GFP protein to confirm whether the bacteria in the fiber were alive or not.

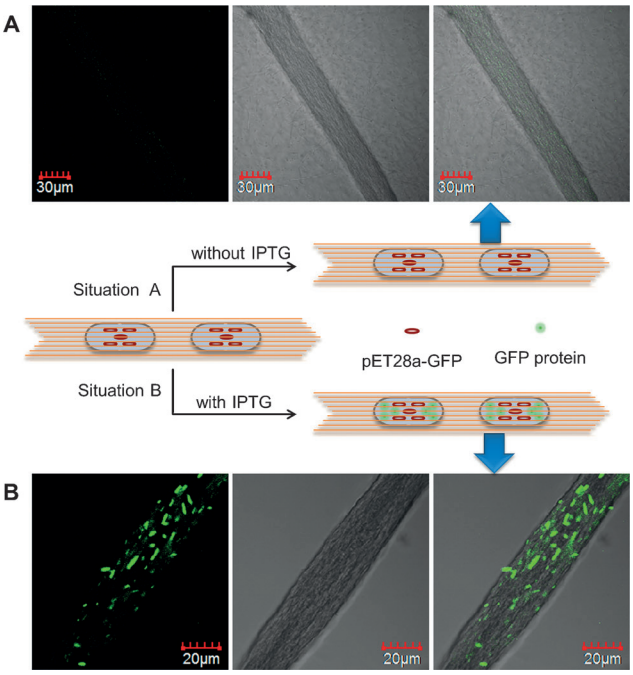

Figure 3. Fluorescent, bright-field, and merged images of IPC fibers encapsulating GFP-coded *Escherichia coli* BL21 by CLSM. These fibers were incubated in the liquid LB culture medium with 50 μg mL^{-1} Kanamycin without (A) and with (B) 25 mg mL^{-1} of IPTG for 4.5 h at 37 °C. GFP emission was collected from 500 to 520 nm. The false color of GFP is green. [DNA] = [H] = 8 mg mL^{-1}, [PT] = 0.4 mg mL^{-1}.

The control experiment without IPTG exhibits that no GFP was expressed in the bacteria (Figure 3 A). After incubation in the liquid LB culture medium with IPTG, the bacteria-occupied region gives a green color as shown in Figure 3 B, which indicates that GFP-coded *Escherichia coli* BL21 encapsulated in the fibers is alive and meanwhile keeps its biological activity. Even after incubation in culture medium for 24 h, the IPC fibers were not broken, which exhibits that they possess good stability in the biological environment. These results display that the fiber has good permeability, and the nutrients required for bacteria growth would diffuse into the fibers. Also, the IPC progress is moderate enough to prevent the encapsulated bacteria from exposing to the external environment of the fibers.

In conclusion, four CCPs have been synthesized with four emission colors (blue, green, orange, and red). These CCPs can respectively form inherent fluorescent microfibers with natural salmon sperm DNA and histone proteins through the interfacial polyelectrolyte complexation procedure. We also obtained color-encoded IPC fibers based on the co-assembly of DNA, histone proteins, and RGB-emissive CCPs. The DNA/histone/CCPs IPC fibers show multi-colored emissions by tuning the FRET efficiencies among CCPs under a single excitation wavelength with large Stokes shifts. The color could be adjusted through fine-tuning the molar ratios of the three CCPs (FRET occurs among them) and twelve color-encoded IPC fibers were obtained. Isothermal titration microcalorimetry (ITC) shows that the driving forces for fiber formation are electrostatic and hydrophobic interac-

tions, as well as the release of counterions and bound water molecules. The DNA/histone/CCPs IPC fibers could encapsulate *Escherichia coli* and the expression of GFP proteins was successfully regulated by external environment. These multi-colored fibers show a great potential in biomedical applications, such as biosensor, delivery and release of biological molecules, and tissue engineering.

Experimental Section

Fiber formation: Salmon sperm DNA, histone proteins (H) and PT were dissolved in water (8 mg mL^{-1} for each polyelectrolyte). Droplets of two oppositely charged polyelectrolyte solutions (5 μL each) were placed adjacent to each other on a plastic Petri dish. The two droplets were then brought in contact with each other by using a pair of tweezers to form a stable interface. The fiber was fabricated by continuously drawing up the interface.

Incorporation of cationic conjugated polymers (CCPs) into the IPC fibers: PFP (1 mM, 0.7 mg mL^{-1}, 5% DMSO aqueous solution), PPE (1 mM, 0.9 mg mL^{-1}, THF), PT (20.9 mM, 8 mg mL^{-1}, H_2O), PBF (5.7 mM, 8 mg mL^{-1}, 20% DMSO aqueous solution) and H (100 mg mL^{-1}, H_2O) were diluted to sterilized water according to the required concentration. The acquired mixtures were used as the positively charged substances to make a fiber.

Incapsulation of *Escherichia coli* in the IPC fibers: GFP-coded *Escherichia coli* BL21 (6 μL) that was just recovered was transferred to 10 mL liquid LB (Luria-Bertani) culture medium and grown at a shaker (37 °C, 180 rpm) overnight. The obtained bacterial suspension (2 mL) was centrifuged and the residue was washed with 1 × PBS for three times. Then the supernatant was discarded and the remaining GFP-coded *Escherichia coli* BL21 were resuspended in sterilized water (50 μL). After that, 8 μL of the resuspended bacterial suspension was added to 42 μL DNA solution (8 mg mL^{-1}), the obtained suspension was used as the negatively charged substance to make a fiber.

Received: October 9, 2013
Published online: November 24, 2013

Keywords: conjugation · DNA · fibers · polymers · proteins

[1] B. Smitha, S. Sridhar, A. A. Khan, *Eur. Polym. J.* **2005**, *41*, 1859 – 1866.
[2] M. Tiitu, J. Laine, R. Serimaa, O. Ikkala, *J. Colloid Interface Sci.* **2006**, *301*, 92 – 97.
[3] A. V. Svensson, L. Huang, E. S. Johnson, T. Nylander, L. Piculell, *ACS Appl. Mater. Interfaces* **2009**, *1*, 2431 – 2442.
[4] Z. Gu, Y. Yuan, J. He, M. Zhang, P. Ni, *Langmuir* **2009**, *25*, 5199 – 5208.
[5] H. Yamamoto, Y. Senoo, *Macromol. Chem. Phys.* **2000**, *201*, 84 – 92.
[6] A. C. A. Wan, I.-C. Liao, E. K. F. Yim, K. W. Leong, *Macromolecules* **2004**, *37*, 7019 – 7025.
[7] a) A. C. A. Wan, M. F. Leong, J. K. C. Toh, Y. Zheng, J. Y. Ying, *Adv. Healthc. Mater.* **2012**, *1*, 101 – 105; b) B. C. U. Tai, C. Du, S. J. Gao, A. C. A. Wan, J. Y. Ying, *Biomaterials* **2010**, *31*, 48 – 57.
[8] J. Yang, G. Balasundaram, S.-L. Lo, E. C. S. Guang, J. Xue, J. Song, A. C. A. Wan, J. Y. Ying, S. Wang, *Adv. Mater.* **2012**, *24*, 3280 – 3284.
[9] S. Razdan, P. K. Patra, S. Kar, L. Ci, R. Vajtai, A. Kukovecz, Z. Konya, I. Kiricsi, P. M. Ajayan, *Chem. Mater.* **2009**, *21*, 3062 – 3071.
[10] S. H. Lim, I.-C. Liao, K. W. Leong, *Mol. Ther.* **2006**, *13*, 1163 – 1172.
[11] a) A. C. A. Wan, B. C. U. Tai, K.-J. Leck, J. Y. Ying, *Adv. Mater.* **2006**, *18*, 641 – 644; b) K. Narayanan, K.-J. Leck, S. Gao, A. C. A. Wan, *Biomaterials* **2009**, *30*, 4309 – 4317; c) S. Z. Yow, C. H. Quek, E. K. F. Yim, C. T. Lim, K. W. Leong, *Biomaterials* **2009**, *30*, 1133 – 1142.
[12] J. Yang, Y. Zhang, S. Gautam, L. Liu, J. Dey, W. Chen, R. P. Mason, C. A. Serrano, K. A. Schug, L. Tang, *Proc. Natl. Acad. Sci. USA* **2009**, *106*, 10086 – 10091.
[13] a) U. Resch-Genger, M. Grabolle, S. Cavaliere-Jaricot, R. Nitschke, T. Nann, *Nat. Methods* **2008**, *5*, 763 – 775; b) P. D. Wadhavane, R. E. Galian, M. A. Izquierdo, J. Aguilera-Sigalat, F. Galindo, L. Schmidt, M. I. Burguete, J. Perez-Prieto, S. V. Luis, *J. Am. Chem. Soc.* **2012**, *134*, 20554 – 20563.
[14] a) C. Zhu, L. Liu, Q. Yang, F. Lv, S. Wang, *Chem. Rev.* **2012**, *112*, 4687 – 4735; b) S. W. Thomas, G. D. Joly, T. M. Swager, *Chem. Rev.* **2007**, *107*, 1339 – 1386; c) H.-A. Ho, A. Najari, M. Leclerc, *Acc. Chem. Res.* **2008**, *41*, 168 – 178; d) H. Jiang, P. Taranekar, J. R. Reynolds, K. S. Schanze, *Angew. Chem.* **2009**, *121*, 4364 – 4381; *Angew. Chem. Int. Ed.* **2009**, *48*, 4300 – 4316; e) U. H. F. Bunz, V. M. Rotello, *Angew. Chem.* **2010**, *122*, 3338 – 3350; *Angew. Chem. Int. Ed.* **2010**, *49*, 3268 – 3279.
[15] a) X. Duan, Z. Li, F. He, S. Wang, *J. Am. Chem. Soc.* **2007**, *129*, 4154 – 4155; b) F. Feng, H. Wang, L. Han, S. Wang, *J. Am. Chem. Soc.* **2008**, *130*, 11338 – 11343; c) Q. Yang, Y. Dong, W. Wu, C. Zhu, H. Chong, J. Lu, D. Yu, L. Liu, F. Lv, S. Wang, *Nat. Commun.* **2012**, *3*, 1206.
[16] a) X. Feng, L. Liu, S. Wang, D. Zhu, *Chem. Soc. Rev.* **2010**, *39*, 2411 – 2419; b) J. Pecher, S. Mecking, *Chem. Rev.* **2010**, *110*, 6260 – 6279; c) A. Kaeser, A. P. H. J. Schenning, *Adv. Mater.* **2010**, *22*, 2985 – 2997; d) K.-Y. Pu, B. Liu, *Adv. Funct. Mater.* **2011**, *21*, 3408 – 3423.
[17] B. Liu, B. S. Gaylord, S. Wang, G. C. Bazan, *J. Am. Chem. Soc.* **2003**, *125*, 6705 – 6714.
[18] H. Chong, C. Nie, C. Zhu, Q. Yang, L. Liu, F. Lv, S. Wang, *Langmuir* **2012**, *28*, 2091 – 2098.
[19] X. Feng, G. Yang, L. Liu, F. Lv, Q. Yang, S. Wang, D. Zhu, *Adv. Mater.* **2012**, *24*, 637 – 641.
[20] Y. Zheng, H. Bai, Z. Huang, X. Tian, F.-Q. Nie, Y. Zhao, J. Zhai, L. Jiang, *Nature* **2010**, *463*, 640 – 643.
[21] a) T. K. Dam, C. F. Brewer, *Chem. Rev.* **2002**, *102*, 387 – 429; b) M. W. Freyer, E. A. Lewis, *Methods Cell Biol.* **2008**, *84*, 79 – 113.
[22] a) M. A. Alam, Y.-S. Kim, S. Ogawa, A. Tsuda, N. Ishii, T. Aida, *Angew. Chem.* **2008**, *120*, 1993 – 1994; *Angew. Chem. Int. Ed.* **2008**, *47*, 1967 – 1968; b) B. Wang, H. Yuan, C. Zhu, Q. Yang, F. Lv, L. Liu, S. Wang, *Sci. Rep.* **2012**, *49*, 766.

